Frequency-tuned microwave photon counter based on a superconductive quantum interferometer

V. I. Shnyrkov

B. Verkin Institute for Low Temperature Physics and Engineering, National Academy of Sciences of Ukraine, 47 Nauky Ave., Kharkiv 61103, Ukraine and The Northwest China Research Institute of Electronic Equipment (NWIEE), No. 30, Zhangba Sanlu, Xi'an, Shaanxi 710065, China

Wu Yangcao

The Northwest China Research Institute of Electronic Equipment (NWIEE), No. 30, Zhangba Sanlu, Xi'an, Shaanxi 710065, China

A. A. Soroka

National Science Center "Kharkiv Institute of Physics and Technology," Akhiezer Institute for Theoretical Physics, 1 Akademicheskaya Str., Kharkiv 61108, Ukraine

O. G. Turutanov[a)] and V. Yu. Lyakhno

B. Verkin Institute for Low Temperature Physics and Engineering, National Academy of Sciences of Ukraine, 47 Nauky Ave., Kharkiv 61103, Ukraine

(Submitted November 2, 2017)
Fiz. Nizk. Temp. **44**, 281–291 (March 2018)

Various types of single-photon counters operating in infrared, ultraviolet, and optical wavelength ranges are successfully used to study electromagnetic fields, analyze radiation sources, and solve problems in quantum informatics. However, their operating principles become ineffective at millimeter band, S-band, and ultra-high frequency bands of wavelengths due to the decrease in quantum energy by 4–5 orders of magnitude. Josephson circuits with discrete Hamiltonians and qubits are a good foundation for the construction of single-photon counters at these frequencies. This paper presents a frequency-tuned microwave photon counter based on a single-junction superconducting quantum interferometer and flux qutrit. The control pulse converts the interferometer into a two-level system for resonance absorption of photons. Decay of the photon-induced excited state changes the magnetic flux in the interferometer, which is measured by a SQUID magnetometer. Schemes for recording the magnetic flux using a DC SQUID or ideal parametric detector, based on a qutrit with high-frequency excitation, are discussed. It is shown that the counter consisting of an interferometer with a Josephson junction and a parametric detector demonstrates high performance and is capable of detecting single photons in a microwave band. *Published by AIP Publishing.*
https://doi.org/10.1063/1.5024538

1. Introduction

Any electromagnetic field, even without taking into account random interference, experiences certain fundamental fluctuations associated with the field itself. The theory of optical coherence provides a statistical description of such fluctuations, and optical coherence effects are the manifestation of correlation between them. Electromagnetic fields of the optical and microwave bands are fundamental carriers of information in classical and quantum communication channels; as a result, the study of this research area has received close attention recently. In particular, the use of single-photon quantum counters is of interest. For example, the quantum cryptography protocol reliability is based on the assumption that the secret code (key) is distributed by single photons.[1]

The paper[2] shows that the use of photon counters allow measurement of the correlation between values that quadratically depend on the electromagnetic field parameters. The second-order correlation function adequately describes the effects of the second and higher orders for statistics of fields created by thermal sources. However, following the development of lasers, further development of the theory was required, in particular, on the basis of quantum-mechanical analysis[3] which provided a complete statistical description of arbitrary optical fields. In turn, the quantum theory predictions, for example, sub-Poisson statistics for photons emitted in the resonance fluorescence of a two-level atom ("anti-bunching")[4] and its experimental confirmation[5] led to the development of single-photon counters in the optical band. Surprising properties of electromagnetic fields were demonstrated in this rapidly developing field: sub-Poisson statistics for lasers with low-noise pumping, squeezed states of light, parametric conversion of the optical photon frequency with the generation of photon pairs, entanglement of the states of individual photons, etc.

At present, solid-state single-photon avalanche diodes (SPADs) cooled down to the nitrogen temperature level and based on semiconductors of the InGaAs, gallium arsenide (GaAs), and indium phosphate (InP) type;[6] superconducting bolometers (TES) with an operating temperature of 0.1 K;[7] and superconducting single-photon detectors (SSPD or

SNSPD) based on ultra-thin niobium nitride films at $T = 2\,K$[8] are known to exhibit the best characteristics at a wavelength range from 0.1 to 6 μm. Semiconductor detectors at quantum dots have been successfully applied for the detection of radiation in the far infrared band.[9,10]

Remarkable achievements in the development of the element base for constructing quantum computers based on superconducting qubits[11,12] suggests the potential for their practical realization, and has resulted in increased efforts towards the development of quantum informatics using electromagnetic fields in the microwave band. Single-photon counters in this band are necessary for both statistical and correlation analyses of fields, and for the creation of hybrid optical-microwave quantum systems. Despite the obvious difficulty that results from the fact that the energy of microwave quanta is 4–5 orders of magnitude less than that of the optical quanta, single-photon counters at frequencies of 3.8 and 10.2 GHz have been proposed and demonstrated in recent papers.[13–16]

Superconducting nonlinear Josephson structures with discrete energy spectra, which are analogs of a single atom, are the basic element for the construction of frequency-selective counters. The existence of discrete energy levels was demonstrated by observations of macroscopic resonance tunneling in a superconducting interferometer,[17] and resonance absorption of microwave power in the electromagnetic field-induced decays of metastable current states in the Josephson junction.[18] For the reasons described below, the characteristic frequencies between the ground $|0\rangle$ and excited $|1\rangle$ energy levels for macroscopic quantum communications with Josephson junctions are in the following range

$$\frac{\omega_{01}}{2\pi} = \frac{\delta E_{01}}{h} \approx 1 - 40\,\text{GHz}.$$

2. Single-photon counter based on Josephson junction

The condition of absence of incoherent mixing of the ground E_0 and excited E_1 energy levels due to thermal fluctuations requires fulfillment of the following stringent condition for the operating temperature of quantum counters: $k_B T \ll \hbar\omega_{01} = E_1 - E_0$. For example, in the case of detection, which is interesting from a practical perspective, of photons with a frequency of $\omega_{01}/2\pi$=10 GHz, this condition leads to $T \ll 0.5$ K, and, assuming $k_B T \approx 0.1\,\hbar\omega_{01}$, we obtain $T \approx 50$ mK. A temperature range of $T = 10$–30 mK is typical for dilution refrigerators.

The possibility of counting single photons in the microwave band (3.8 GHz) by a Josephson junction with a discrete Hamiltonian has been successfully demonstrated.[15] However, the application of this option for constructing a counter is limited by considerable difficulties associated with increasing the photon frequency and, above all, the long recovery time of the equilibrium state τ, which should pass before the registration of the next photon. In addition, suppression of the "electromagnetic temperature" of communications conductively-coupled with a Josephson junction requires their thorough broadband filtering[18] to reduce "dark" readings. Nevertheless, despite the indicated difficulties, photon counters based on Josephson junctions are promising due to the simplicity of the chain of detectors in this approach. Let us briefly consider the basic requirements for the Josephson junction, which are necessary for creating a counter for microwave photons.

A tunneling Josephson junction at low temperatures ($T \ll T_c$) is described by three main parameters: critical current I_c, intrinsic capacitance C, and quasiparticle resistance $R_{qp}(V)$, depending on the voltage across the junction V. According to the scheme of the microwave photon detector, the junction is conductively-coupled with signal control and recording circuits, which may be represented at these frequencies in the form of capacity of circuits $C_c \approx 1$ pF and resistance R_c, connected in parallel to the junction. Since $Rc \ll R_{qp}(V)$, the junction behavior is well described by the resistance model[19,20] with $R \cong R_c \approx 100\,\Omega$. In the superconducting state, when the transport current $I < I_c$, the one-dimensional potential curvature

$$U(\varphi) = \left(\frac{I_c \Phi_0}{2\pi}\right)\left[\cos\varphi + \left(\frac{I}{I_c}\right)\varphi\right], \qquad (1)$$

for the motion of a particle of weight $C(\Phi_0/2\pi)^2$ decreases rapidly when approaching the critical current $I \cong I_c$, where $\Phi_0 = h/2e$ is magnetic flux quantum and φ is the phase difference at Josephson junction. This results in the dependence of plasma frequency $\omega_P(I)/2\pi$ on transport current[19]

$$\omega_P(I) = \omega_{p0}\left[1 - \left(\frac{I}{I_c}\right)^2\right]^{1/4}, \qquad (2)$$

where $\omega_{P0} = [2\pi I_c/(\Phi_0 C)]^{1/2}$. A conductive coupling in such circuit engineering limits the oscillator quality factor $Q = \omega_P(I)RC$ with R value; in order to fulfill the condition $Q \geq 10$, the use of junctions with a sufficiently high intrinsic capacitance $C \geq 10$ pF is required.[15] In practice, this leads to a decrease in the typical impedance of a Josephson junction $Zj = (Lj/C)^{1/2}$, fulfillment of condition $C \gg C_c$, and a decrease in the plasma frequency in proportion to $C^{-1/2}$.

There is a large number [approximately $Ic\Phi 0/(2\pi\hbar\omega 01)$] of energy levels in the quantum limit at $I = 0$ in the potential (1). The initial state of the counter with two energy levels E_0 and E_1 is obtained by passage of pulse current with the amplitude of $I \cong I_c$ with a typical buildup time of 1–5 ns. The relative accuracy of setting the pulse generator amplitude should be $\sim 10^{-5}$ due to the large number of levels. The system will be in the ground state E_0 under adiabatic conditions. A photon-induced transition to the excited E_1 level will occur after the resonance absorption of the microwave band energy quantum $\hbar\omega_{01} \cong E_1 - E_0$ by a counter, and the system will possibly enter the resistive area ($\varphi \neq 0$) with a voltage of ~ 1 mV appearing at the junction. This is the reading of a single quantum by the counter; moreover, the probability density of transition to the resistive area from the E_1 level has both tunneling (MKT) and classic components.[20] The height of the potential barrier (1) separating the superconducting and resistive states, as well as the value $E_1 - E_0$, depend on the transport current amplitude. It is important to select the potential barrier by passing the transport current in such a way that the relaxation rate ($\sim 1/RC$) from the E_1 level to the ground E_0 level would be significantly less than the

transition rate to the resistive state. The values of Josephson coupling energy $Ej = I_c\Phi_0/2\pi$ and plasma frequency $\omega_P(I) \sim \sqrt{I_c/C}$ may be controlled (reduced) by the application of external magnetic field using classic dependency $I_c(H)$ for the SIS junction.[20]

The change rate φ of phase difference in the photon counter in the quasiclassical region $\varphi \neq 0$ is determined by the parameter indicating attenuation

$$\beta_c = 2\pi I_c R^2 C \Phi_0^{-1} \gg 1. \quad (3)$$

For example, for the above mentioned parameters $R \approx 100\ \Omega$, $C \approx 10$ pF, and junction critical current $I_c = 10\ \mu$A, the β_c value exceeds 3000. This means that, after measuring the voltage in order to return the counter to the superconducting state, the transport current should be rapidly reduced to zero. Joule heat is released in the Josephson junction in the quasiclassical region due to dissipative processes, and its temperature may exceed the refrigerator temperature, as the relaxation rate to the equilibrium state decreases at low temperatures $T = 10$–30 mK. Therefore, even after the counter enters the superconducting state $\varphi = 0$, an additional time τ is required to reach the equilibrium state. It is difficult to reduce this time to less than 1 ms; in the experiment, it determines the time interval between the recording of individual photons.

The indicated limitations of the photon counter based on single contact may be eliminated by including it in the superconducting ring. Absence of conductive coupling in this case allows improved isolation of the counter from control circuits and signal recording, making the system, in a certain sense, "more quantum." For brevity, such a topology will be referred to as "HF SQUID," implying that this is a superconducting quantum interferometer with geometric inductance $L < L_F = (\Phi_0/2\pi)^2(k_BT)^{-1}$.

3. HF SQUID with adjustable critical current for a single-photon counter

If an external magnetic flux Φ_e is applied to the HF SQUID, a screening current $I_s = -I_c \sin(2\pi\Phi/\Phi_0)$ is induced in it (here Φ—total flux in the SQUID ring, $\Phi = \Phi_e + LI_s$). The equation for the classical motion Φ (taking into account the possible dissipation R^{-1}) is equivalent to the equation describing a particle with the weight of C in the potential $U(\Phi, \Phi_e)$

$$C\ddot{\Phi} + \frac{\dot{\Phi}}{R} = -\frac{\partial U(\Phi, \Phi_e)}{\partial \Phi}. \quad (4)$$

Here R—total equivalent resistance shunting the Josephson SIS junction. The potential $U(\Phi, \Phi_e)$ for the HF SQUID can be represented as the sum of magnetic energy and Josephson coupling energy

$$U(\Phi,\ \Phi_e) = U_0\left[0.5(\varphi - \varphi_e)^2 + \beta_L \cos\varphi\right], \quad (5)$$

where $\varphi = 2\pi\Phi/\Phi_0$, $\varphi_e = 2\pi\Phi_e/\Phi_0$ are internal and external magnetic fluxes, respectively, $U_0 = \Phi_0{}^2/4\pi^2L$, $\beta_L = 2\pi LI_c/\Phi_0$. The φ value is also the phase difference on the Josephson junction [see (1)]. The parameters L, R, C, β_L, and Φ_e completely describe the potential and equation for the classical motion of the flux Φ. Let us consider the case of existence of two metastable states in order to analyze of photon counter based of the HF SQUID. It follows from (5) that the system will have a symmetric double-well potential $U(\Phi)$ in the case of external flux $\Phi_e = \Phi_0/2$ for the values $1 < \beta_L < 4.6$, in which the "left" and "right" wells correspond to the two fluxoid states of the HF SQUID. These states correspond to persistent currents in the HF SQUID moving in opposite directions.

In order to construct a photon counter it is convenient (within these limits) to have the ability to control the height of potential barrier separating the two states *in situ*. This scheme was first used to observe the quantum superposition of individual states,[21] where a single Josephson junction was replaced by a DC SQUID with low inductance l, closed by contacts with critical currents $i_{c1} \cong i_{c2}$.[22–25] Generally, two contacts in a ring imply movement along two coordinates. However, if the strong inequality $l \ll L$ is satisfied, for example, l is 2–3% of L, and $\beta l < 1$, the DC SQUID in the B photon detector (Fig. 1) can be considered as a Josephson junction with double capacitance (weight) and adjustable critical current $I_{c\max} \approx 2i_c$. The dimensionless inductance value in such configuration will depend on the control current $\beta_L = \beta_{L\max}\cos(\pi M_{g1}I_{g1}/\Phi_0)$, where $\beta_{L\max}$—maximum parameter value at $M_{g1}I_{g1} = n\Phi_0$. Small M_{g1}, M_{g2}, M_q values (Fig. 1) are selected to reduce the noise from filters in the control circuits.

DC SQUIDs with the energy sensitivity of $\delta E\ \delta t \sim \hbar$ are usually used for quantum measurements of magnetic flux variations in such schemes.[21–25] However, the proper (Josephson) oscillation from the DC SQUID in the operating point (with a large conversion coefficient) may not only form "dark" readings, but also lead to complete mixing of the quantum system intrinsic energy levels. In order to reduce these effects, it is necessary to carefully screen the qubit from the measuring circuit with a high-resistance shield. Let us note an interesting proposal[26] that allows significant reduction of the indicated effects due to the use of INSQUID (INductive Superconducting QUantum Interference Device) scheme, in which DC SQUID may be "disconnected" (i.e., to prevent interaction of device with the measured quantum system) and

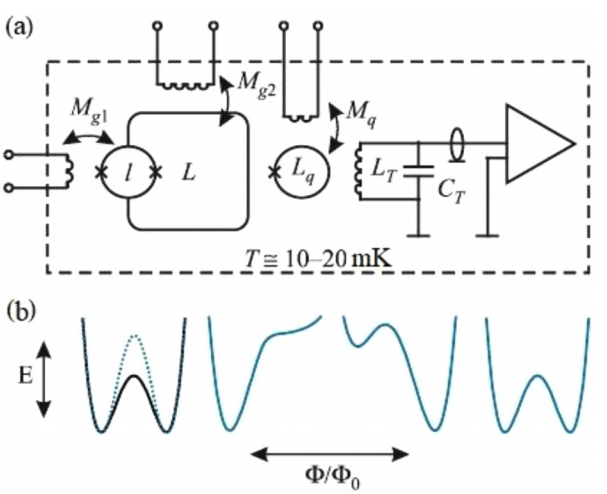

Fig. 1. (a) Block schematic diagram of a microwave photon counter based on a HF SQUID with an adjustable potential barrier and a parametric qutrit detector of magnetic flux. $M_{g1} \approx 0.15$ pH; $M_{g2} \approx 1.5$ pH; $Mq \approx 1.0$ pH; $L \approx 200$ pH; $l \approx 6$ pH; $Lq \approx 100$ pH. (b) A family of potential energy profiles in controlling the barrier height (dashed line) *via* the gate M_{g1} and installation of the counter *via* the gate M_{g2}.

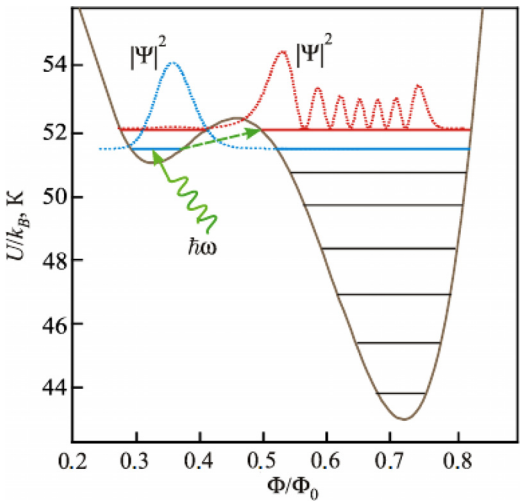

Fig. 2. The double-well potential and energy levels of the photon counter with the parameters $L = 2 \times 10^{-10}$ H, $\beta_L = 1.325$, and $C = 76$ fF after installation at the point $\Phi_e = 0.5135\ \Phi_0$. Squares of wave functions are shown for two operating levels of the counter.

"connected" for the measurement time. In this paper, we consider (Fig. 1) an almost "perfect" broadband parametric magnetic flux detector based on qutrit[27] for continuous reading of states in a photon counter.

3.1. Photon counter in the flux qubit mode

The quantum behavior of the macroscopic variable Φ may be analyzed by considering the Hamiltonian of an isolated HF SQUID. The Hamiltonian has the following form in a system without attenuation at $T = 0$

$$H(\Phi, \Phi_e) = \frac{Q^2}{2C} + U(\Phi, \Phi_e). \tag{6}$$

Photon counter β_L values with adjustable barrier are determined by the superconducting current of the DC SQUID and are dependent on the control flux of the gate M_{g1}; the external flux Φ_e is set by the gate M_{g2} (Fig. 1). The charge Q and the magnetic flux Φ are connected by the commutation relation $[\Phi, Q] = i\hbar$. Typical values of the energy levels in the flux qubit can be obtained by solving the steady Schrödinger equation with the Hamiltonian (6)

$$\left\{ -\frac{\hbar^2}{2C}\frac{\partial^2}{\partial\Phi^2} + \left(-\frac{I_c\Phi_0}{2\pi}\cos 2\pi\frac{\Phi}{\Phi_0} + \frac{(\Phi - \Phi_e)^2}{2L} \right) \right\} \Psi(\Phi) = E\,\Psi(\Phi). \tag{7}$$

After converting to dimensionless variables,

$$x = \frac{\Phi}{\Phi_0} = \frac{\varphi}{2\pi}, \quad x_e = \frac{\Phi_e}{\Phi_0} = \frac{\varphi_e}{2\pi}, \quad M \equiv \frac{k_B\Phi_0^2}{\hbar^2}C$$

and standardizing the energies to the Boltzmann constant k_B, the Schrödinger equation can be obtained in the following form:

$$\left\{ -\frac{1}{2M}\frac{\partial^2}{\partial x^2} + U(x) \right\} \Psi(x) = \varepsilon\,\Psi(x), \tag{8}$$

where $U(x) = U_0\ [-\beta\ \cos 2\pi x + 2\pi^2(x - xe)^2]$ is the particle motion potential and $U_0 \equiv (\Phi_0/2\pi)/(k_B L)$ is the typical energy determined by the counter inductance L.

Solutions of Eq. (8) depend on the intrinsic capacitance of contacts and on the dimensionless parameter β_L value.

Energy spectra in a double-well potential for a photon counter with parameters $L = 2 \times 10^{-10}$ H, $\beta_L = 1.325$, and $C = 76$ fF, obtained by a numerical solution of (8) at the point $\Phi_e = 0.5135\ \Phi_0$ are presented in Fig. 2. Squares of wave functions are shown for the ground and excited levels. It is apparent that the magnetic flux average value in the counter changes by approximately $0.4\ \Phi_0$ after the photon-induced transition.

Figure 3(a) shows dependencies of distance between the two ground levels of the photon counter in units of frequency $f = (E_1 - E_0)/h$ on the external magnetic flux set *via* the gate M_{g2}, for the three values of dimensionless parameter β_L (gate M_{g1}). The frequency tuning range of the two-level system increases with the HF SQUID critical current growth. A decrease in the total capacitance of the photon detector results in an increase in characteristic frequency, which should be expected from the general dependence $f \sim (LC)^{-1/2}$. Hence, it follows that, by decreasing the capacitance of

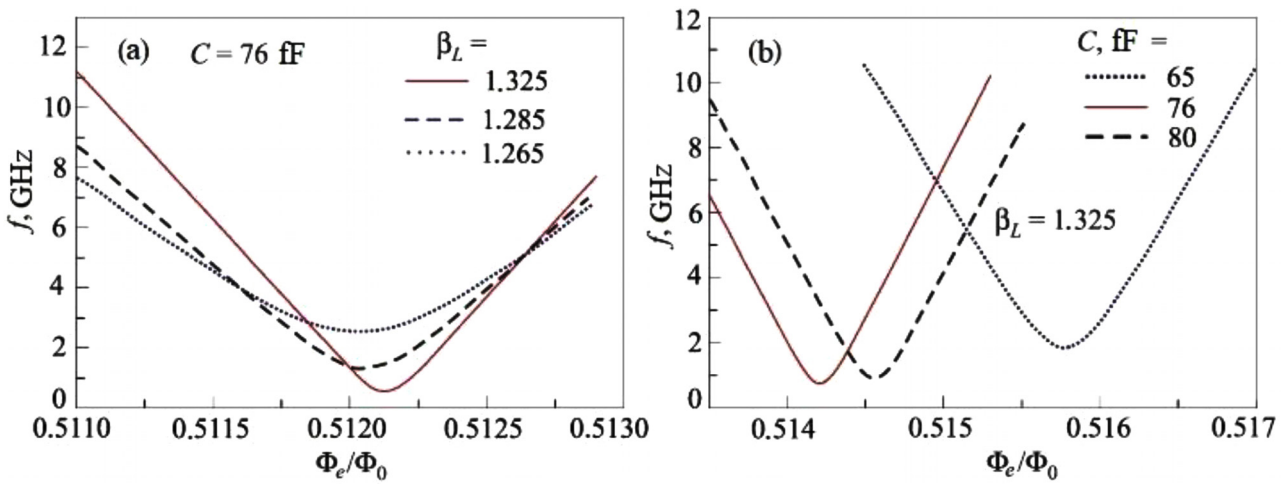

Fig. 3. A family of dependencies of the characteristic frequency f of a two-level system of the photon counter on the external magnetic flux Φ_e, set *via* the gate M_{g2}. Family parameters: (a) dimensionless critical current β_L, (b) intrinsic capacitance C values of the counter.

Josephson junctions and adjusting the dimensionless critical current of the HF SQUID, the resonant excitation of the photon detector maybe shifted to the high-frequency region of 10–30 GHz.

It should be noted that the wave function $|\Psi\rangle$ for an isolated quantum system in the pure limit is always a linear superposition of several states $|\Psi\rangle = \sum_i c_i |a_i\rangle$, where $|c_i|^2$—complex numbers corresponding to the probability amplitude of observation of the intrinsic state $|a_i\rangle$.

The coherent superposition of current states in the three-well potential was first observed by a group of researchers from Kharkiv[28] in 1985. The difficulty lies in the interpretation of the simultaneous measurement of three coefficients $|c_i|^2$ dependent on the external flux. It is usually considered that, when measurement is performed, the wave function "collapses" into one of the eigenvalues. Previous studies[29,30] demonstrate that the performance of weak continuous measurements at a macroscopic level can determine the macroscopic quantum system state with an arbitrarily small perturbation of its intrinsic dynamics. The results of detailed theoretical analysis of the dynamics of superposition states in the three-well potential of HF SQUID[27] completely agree with the experimental data[28] obtained by this method. The almost perfect parametric detector based on qutrit with SIS junction described below makes it possible to construct a magnetic flux detector for continuous fuzzy quantum measurements of a photon counter based on a flux qubit. In fact, the scenario for measuring the photon absorption event by a qubit, considered in Ref. 16, differs from our consideration only in the regenerative circuit of signal recording (with internal pumping), while we register changes in the amplitude (phase) of oscillations in a nonlinear resonator (with external pumping).

3.2. Photon counter based on HF SQUID with dissipation

In general, design of the input circuits and gates of the photon counter based on a HF SQUID may contain dissipative elements that introduce attenuation proportional to the coupling coefficient α. This essentially modifies quantum phenomena in a macroscopic oscillator.[31–34] For example, it was shown in these papers that consideration of attenuation leads to a shift in the intrinsic frequency (energy levels) of a HF SQUID, an exponential attenuation of coherent phenomena in the double-well potential of photon counter, and a decrease in the tunneling rate between these individual states. These theoretical results are sufficiently general and may be used to analyze the destruction of coherence in quantum systems with different dissipation mechanisms.

The final temperature value will not lead to a significant change in the pattern of levels in the photon detector in the mixed state, if the condition $hf \gg k_B T$, is assumed to be fulfilled. However, temperature consideration may affect the rate of decay of metastable current states. If the total attenuation from the control circuits and filters in the counter is characterized by resistance R, then its consideration leads to a shift and broadening of the quantum energy levels. Broadening of levels is proportional to the reciprocal quality factor Q^{-1} of the photon counter, which depends on the intrinsic frequency of the oscillator ω_P, contact capacitance C, and resistance R, $Q = \omega_P RC$.

Assuming the frequency $\omega_P \sim 10$ GHz, $C \sim 7 \times 10^{-14}$ F, and $R \sim 10^3$ Ω for the contacts considered above, we obtain $Q \approx 45$. The distance between the energy levels in the photon counter $hf = E_1 - E_0$ significantly exceeds the intrinsic width of the levels δE_i in the case of such parameters. The shift of levels due to the presence of attenuation is small (proportional to Q^{-2});[35] this may be neglected in the considered case.

Smaller amplitudes of the control pulses are required for the installation of the photon counter to the initial state with a decrease in the number of levels.

This allows improved filtration of circuits and decreases the generation of high-frequency components from the control pulse. Figure 4 demonstrates the scheme of double-well potential of photon counter with $\beta_L = 1.18$, $C \approx 106$ fF, and $L = 0.36$ nH, which contains two levels in the right and left wells.

The initial state (the lower level in the left well) is inverted in relation to the lower level in the right well. However, the relaxation times of the inverse system under such barriers are sufficiently large (milliseconds), and can be disregarded. The relaxation time inside the well is determined by the product RC and is ~1 ns at the selected parameters.

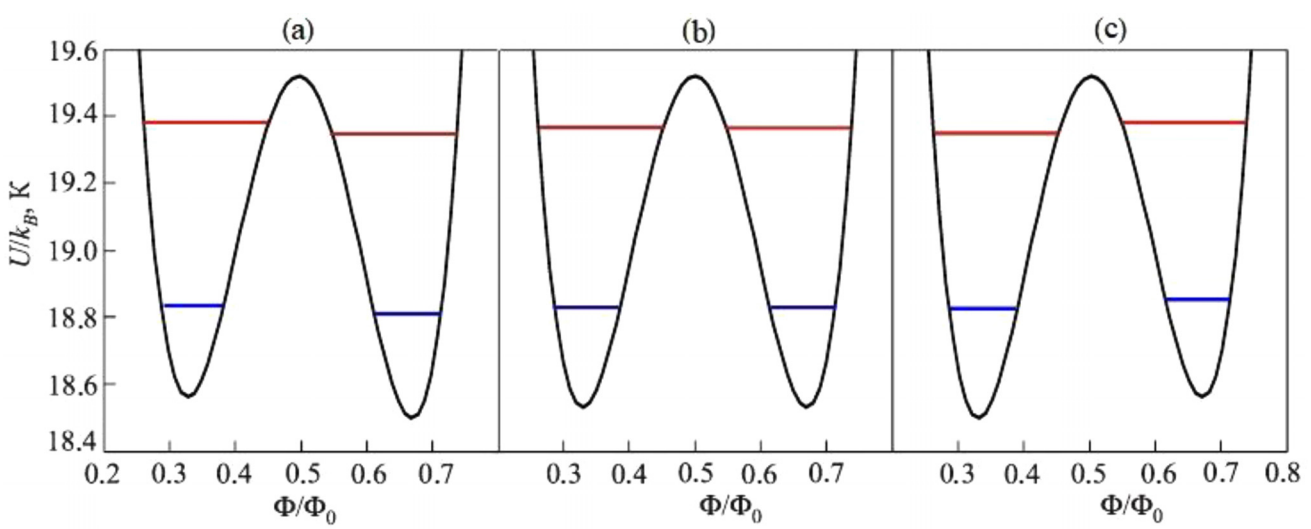

Fig. 4. A family of potentials for a photon counter with two energy levels in each well. Typical distance between levels $(E_1 - E_0)/k_B = 0.5$ K, $\beta_L = 1.18$. Family parameter is the external flux Φ_e value equal to 0.5003 Φ_0 (a), 0.5 Φ_0 (b), and 0.4997 Φ_0 (c).

4. Magnetometer for reading the state of counter based on qutrit

The principle of operation of superconducting parametric magnetic flux detectors based on qubit and qutrit was considered in previous studies.[27,36] The time of establishment of the superposition state $t = \pi\hbar/[2(E_1 - E_0)]$ is several times smaller than with the SIS junction due to the specific form of potential energy in the ring closed by the ScS junction. This enables the use of higher excitation frequencies and increases the performance while creating the parametric magnetic flux detector and remaining in adiabatic mode.

However, SIS junctions are preferable for the development of integrated circuits in terms of modern thin-film technology. Therefore, the main characteristics of superconducting qutrit detector (SQUTRID) of magnetic flux with tunnel Josephson junctions of the SIS type are discussed below.

Method and equations equivalent to Ref. 27 were used during numerical calculations of the SQUTRID characteristics. Let us consider a more general case of nonresonant tunneling. Figure 5(a) shows the three-well potential and square of the wave function for the ground superposition energy level E_{S0} of the SQUTRID at whole-number values of $\Phi_e = n\Phi_0$ of the external flux. The contact capacitance $C = 15$ fF and $\beta_L = 4.8$ are selected in such a way as to minimize possible transitions from the E_{S0} to the excited level E_{S1}. It should be noted that, in this case, the level E_{S-1} located in the middle well is distant from the E_{S0} by more than 4 K. Submicron Josephson junctions with a high critical current density of ~4000 A/cm^2 are required to fulfill these conditions and to create a three-well potential.

Dependence $E_{S0}(\Phi_e)$ shown in Fig. 5(b) demonstrates that the local curvature of the ground superposition level changes significantly at a scale of ~0.01 Φ_0. The influence of fluctuations on the qutrit characteristics is very important in this case. The noise magnetic flux uncertainty associated with the temperature $\langle\Phi_N^2\rangle = k_B L_q T$ should be substantially less than this value in order to observe the typical curvature of the energy level. With reasonable parameters: $T = 10$ mK and $L_q = 0.1$ nH, we obtain $\langle\Phi_N^2\rangle^{1/2} \approx 1.8 \times 10^{-3}\ \Phi_0$. As the detection of single photons in the microwave band is a part of unique experiments using complex equipment, it is possible to count on lower T and L_q values. The reverse effect of the measuring circuit on the ground energy level curvature (quantum inductance L_Q) can be analyzed assuming that the noise spectrum lies well below the frequency of energy exchange between the wells and above the SQUTRID excitation frequency. In this approximation, the quantum inductance of the E_{S0} level may be obtained by averaging over thermodynamic (quasi-stationary) fluctuations.[37]

Figure 6(a) shows a family of dependencies of standardized inverse quantum inductances[27,38–40] on the external magnetic flux Φ_e for various values of its standard deviation σ, obtained in the Gaussian noise distribution approximation. Here, $\sigma^2 = \langle\delta x_e^2\rangle$ is the dispersion of noise flux affecting the qutrit from the measuring circuit (Fig. 1) consisting of a resonant circuit and a cooled amplifier. The conversion slope of a superconducting parametric detector based on qutrit is proportional to the derivative $\partial(L_q/L_Q)/\partial x_e$ whose value (2×10^5) remains sufficiently high [Fig. 6(b)] even at $\sigma = 0.002$. In order to obtain such values and construct detectors based on the quantum inductance of qutrits and qubits, their careful isolation from the external environment is necessary.[41]

The most important characteristics of the parametric magnetic flux detector in the single-quantum photon counter scheme are its own sensitivity, performance (band), and inverse effect on the measured two-level system.[38,42] The inverse quantum inductance derivative values obtained [Fig. 6(b)] at $\sigma = 0.002$–0.003 demonstrate that the conversion slope of a superconducting SQUTRID with the an excitation frequency of 1 GHz can reach 10^{11}–10^{12} V/Wb. This enables consideration the contribution of the amplifier intrinsic noise to the sensitivity, and in some cases, the partial inclusion of the amplifier in the resonant circuit. According to the analysis performed in a previous study,[43] the HF SQUTRID sensitivity in our case is mainly determined by the resonant circuit noise. Such a conclusion can also be made on the basis of the theory developed for calculating the sensitivity of classical HF SQUIDs in the anhysteretic mode,[44] which describes well the experimental results obtained in the paper.[45]

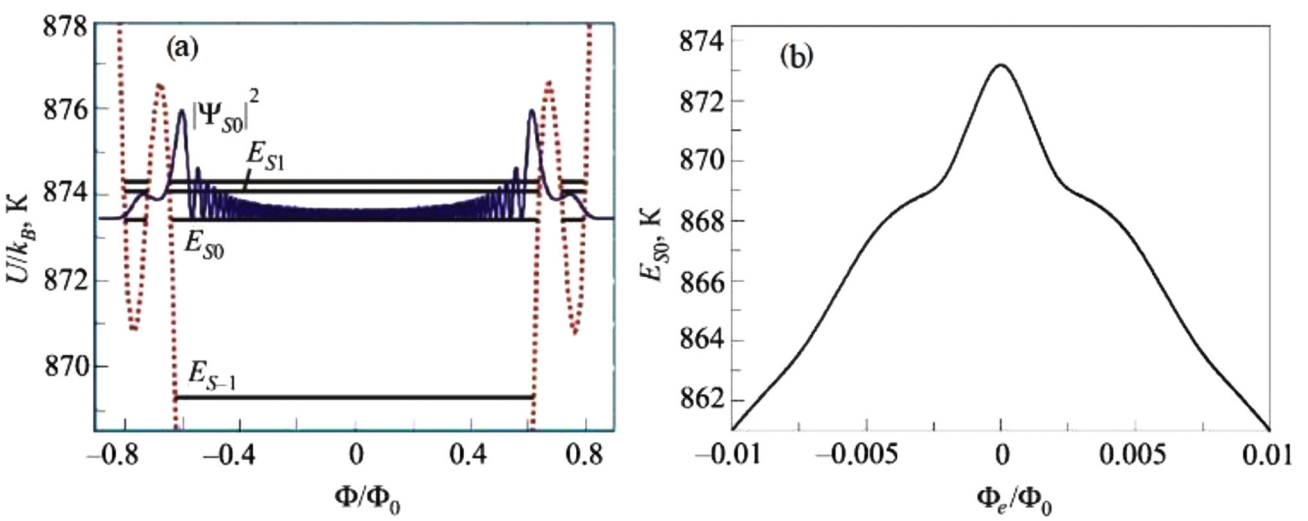

Fig. 5. Superposition of states in a flux qutrit with a Josephson SIS junction. Calculation was carried out with a geometric inductance $L_q = 0.1$ pH, contact capacitance $C = 15$ fF, and $\beta_L = 4.8$. (a) Ground superposition level E_{S0} ($n = 111$) in the three-well potential and the corresponding square of the wave function at the external flux $\Phi_e = n\Phi_0$. (b) Dependence of the ground superposition level E_{S0} energy on the external flux Φ_e. The energies are expressed in temperature units.

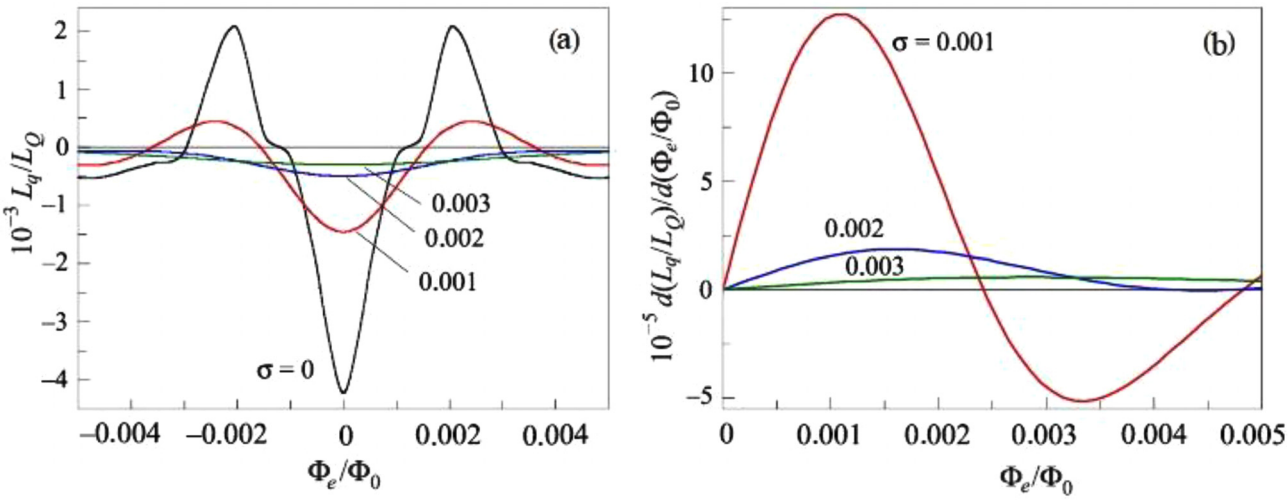

Fig. 6. Families of dependencies of standardized inverse quantum inductances (a) and their derivatives (b) on the external magnetic flux Φ_e at various standard deviations of the noise flux σ. Qutrit parameters correspond to the values presented in Fig. 5.

The first amplifier stage is generally installed in the dilution refrigerator at a temperature of ~1 K due to the large power consumption ($P_{dc} \geq 0.1$ mW). This leads to effective noise temperatures of the resonant circuit ~0.3–0.5 K. An amplifier with extremely low values of $P_{dc} \approx 1$ μW and amplification factor of 10 dB for frequencies up to 0.5 GHz was developed in a previous study[42] in order to reduce the circuit temperature. Taking into account the high cooling capacity of modern dilution refrigerators, one or two of such amplifier stages may be installed directly at a temperature of 10 mK to reduce the resonant circuit noise temperature by a factor of 20–30. With the aid of theoretical models and results obtained in Refs. 43–45, it is possible to estimate the sensitivity of the HF SQUTRID with SIS junction, inductance $L_q = 0.1$ nH at $T = 1$ mK and excitation frequency ~0.4 GHz. The "differential" SQUTRID characteristics are more significant in the considered case than the characteristics averaged by the LFO modulation. Therefore, the excitation amplitudes do not exceed 10^{-3} Φ_0. With an integration time of 1 s, we obtain the magnetic flux resolution $\delta\Phi_{\min} \approx 4 \times 10^{-7}$ Φ_0, which leads to an energy sensitivity $\delta\varepsilon_{\min} \approx 3 \times 10^{-33}$ J/Hz. It is possible to reduce the inverse effect of the HF excitation current on the measured photon detector due to the coupling. If the transformation ratio of the magnetic flux between the HF SQUTRID and the counter is adjusted to 1/200, and the change of flux in the counter by 0.3–0.4 Φ_0 (by ~10^{-3} Φ_0 in SQUTRID) after the microwave quantum absorption is taken into account, we obtain the estimate for the band (performance) of photon detector $\Delta B \approx 4$ MHz at a signal-to-noise ratio of about 2.

Conclusion

The scenario considered above, involving the construction of a microwave photon counter, has two advantages that are typical for rapid single flux quantum logic. First, resistive region typical for the counter based on an autonomous Josephson junction and associated processes of heat release are absent in the case of using the topology of a superconducting interferometer. Second, inductive coupling with the signal control and reading gates allows improved isolation of the counter from the external environment.

The recently obtained results for cryogenic amplifiers with a microwatt power consumption demonstrate[46,47] that operating frequencies can be substantially increased in the case of development of the circuit engineering of semiconductor amplifiers on a modern element base. However, the excitation frequency (and performance) of the photon counter with the detector based on the HF SQUTRID/SQUBID[36] have a natural limitation associated with the adiabatic condition, with respect to the energy exchange rate between the individual states in the qutrit/qubit. In general, transparency in the case of two barriers can be increased due to a decrease in the contact capacitance and under resonance conditions that are considered in a previous work.[27] The latter condition requires a high accuracy of parameter selection, in this case, the capacitance and critical current of the Josephson junction.[28] The frequency of energy exchange in qutrit/qubit can be increased up to ~15 GHz with the actual thin-film technology of Josephson SIS junctions. The excitation frequency in this case can be doubled and be equal to 0.8–1 GHz, which will allow increase of the band (performance) of the microwave photon counter up to 10–20 MHz.

[a]Email: turutanov@ilt.kharkov.ua

[1]N. Gisin, G. Ribordy, W. Tittel, and H. Zbinden, Rev. Mod. Phys. **74**, 145 (2002).
[2]R. Hanbury Brown and R. Q. Twiss, Nature **177**, 27 (1956); **178**, 1046 (1956).
[3]R. J. Glauber, Phys. Rev. **130**, 2529 (1963).
[4]H. J. Carmichael and D. F. Walls, J. Phys. B: At. Mol. Phys. **8**, L77 (1975).
[5]H. J. Kimble, M. Dagenais, and L. Mandel, Phys. Rev. Lett. **39**, 691 (1977).
[6]W. J. Kindt, "Geiger mode avalanche photodiode arrays for spatially resolved single photon counting," Ph.D. thesis (Delft University Press, Delft, The Netherlands, 1999).
[7]D. A. Bennett, D. S. Swetz, D. R. Schmidt, and J. N. Ullom, Phys. Rev. B **87**, 020508(R) (2013).
[8]G. N. Gol'tsman, O. Okunev, G. Chulkova, A. Lipatov, A. Semenov, K. Smirnov, B. Voronov, and A. Dzardanov, Appl. Phys. Lett. **79**, 705 (2001).
[9]S. Komiyama, O. Astafiev, V. Antonov, T. Kutsuwa, and H. Hirai, Nature **403**, 405 (2000).
[10]S. Gustavsson, M. Studer, R. Leturcq, T. Ihn, K. Ensslin, D. C. Driscoll, and A. C. Gossard, Phys. Rev. Lett. **99**, 206804 (2007).

[11]H. Paik, D. I. Schuster, L. S. Bishop, G. Kirchmair, G. Catelani, A. P. Sears, B. R. Johnson, M. J. Reagor, L. Frunzio, L. I. Glazman, S. M. Girvin, M. H. Devoret, and R. J. Schoelkopf, Phys. Rev. Lett. **107**, 240501 (2011).
[12]C. Rigetti, S. Poletto, J. M. Gambetta, B. L. T. Plourde, J. M. Chow, A. D. Córcoles, J. A. Smolin, S. T. Merkel, J. R. Rozen, G. A. Keefe, M. B. Rothwell, M. B. Ketchen, and M. Steffen, Phys. Rev. B **86**, 100506(R) (2012).
[13]G. Romero, J. J. García-Ripoll, and E. Solano, Phys. Rev. Lett. **102**, 173602 (2009).
[14]B. R. Johnson, M. D. Reed, A. A. Houck, D. I. Schuster, L. S. Bishop, E. Ginossar, J. M. Gambetta, L. DiCarlo, L. Frunzio, S. M. Girvin, and R. J. Schoelkopf, Nat. Phys. **6**, 663 (2010).
[15]Y. F. Chen, D. Hover, S. Sendelbach, L. Maurer, S. T. Merkel, E. J. Pritchett, F. K. Wilhelm, and R. McDermott, Phys. Rev. Lett. **107**, 217401 (2011).
[16]K. Inomata, Zh. Lin, K. Koshino, W. D. Oliver, J. S. Tsai, T. S. Yamamoto, and Ya. Nakamura, Nat. Commun **7**, 12303 (2016).
[17]I. M. Dmitrenko, V. A. Khlus, G. M. Tsoi, and V. I. Shnyrkov, LTP **11**, 146 (1985) [Sov. J. Low Temp. Phys. **11**, 77 (1985)].
[18]J. M. Martinis, M. H. Devoret, and J. Clarke, Phys. Rev. B **35**, 4682 (1987).
[19]T. A. Fulton and L. N. Dunkleberger, Phys. Rev. B **9**, 4760 (1974).
[20]K. K. Likharev and B. T. Ul'rikh, *Systems with Josephson Junctions* (MSU Publishing House, Moscow, 1978).
[21]J. R. Friedman, V. Patel, W. Chen, S. K. Tolpygo, and J. E. Lukens, Nature **406**, 43 (2000).
[22]S. Han, J. Lapointe, and J. Lukens, in *Activated Barrier Crossing*, 1st ed. edited by G. Fleming and P. Hänggi (World Scientific, Singapore, 1993), Chap. 9, p. 241.
[23]V. Patel, W. Chen, V. Pottorf, and J. E. Lukens, IEEE Trans. Appl. Supercond. **15**, 117 (2005).
[24]M. G. Castellano, F. Chiarello, R. Leoni, G. Torrioli, P. Carelli, C. Cosmelli, M. Khabipov, A. B. Zorin, and D. Balashov, Supercond. Sci. Technol. **20**, 500 (2007).
[25]S. Poletto, F. Chiarello, M. G. Castellano, J. Lisenfeld, A. Lukashenko, C. Cosmelli, G. Torrioli, P. Carelli, and A. V. Ustinov, New J. Phys. **11**, 013009 (2009).
[26]J. Clarke, T. L. Robertson, B. L. T. Plourde, A. García-Martinez, P. A. Reichardt, D. J. Van Harlingen, B. Chesca, R. Kleiner, Y. Makhlin, and G. Schönat, Phys. Scr. T **102**, 173 (2002).
[27]V. I. Shnyrkov, A. A. Soroka, and O. G. Turutanov, Phys. Rev. B **85**, 224512 (2012).
[28]I. M. Dmitrenko, G. M. Tsoi, and V. I. Shnyrkov, in *2nd All-Soviet Union Conference "Quantum Metrology and Fundamental Physical Constants,"* (Scientific Development and Production Center "Russian Research Institute of Metrology named after D. I. Mendeleev", 1985), p. 81; V. I. ShnyrkovG. V. Tsoi, D. A. Konotop, and I. M. Dmitrenko, in *Proceedings of the 4th International Conference SQUID'91*, Berlin, Federal Republic of Germany, June 18–21, edited by H. Koch and H. Lübbig (1991), p. 211.
[29]A. Leggett and A. Grag, Phys. Rev. Lett. **54**, 857 (1985).
[30]A. N. Korotkov and D. V. Averin, Phys. Rev. B **64**, 165310 (2001).
[31]W. Zurek, Phys. Today **44**(10), 36 (1991).
[32]W. G. Unruh and W. H. Zurek, Phys. Rev. D **40**, 1071 (1989).
[33]A. J. Leggett, S. Chakravarty, A. T. Dorsey, M. P. A. Fisher, A. Garg, and W. Zwerger, Rev. Mod. Phys. **59**, 1 (1987).
[34]S. Chakravarty and A. J. Leggett, Phys. Rev. Lett. **52**, 5 (1984).
[35]W. Bialek, S. Chakravarty, and S. Kivelson, Phys. Rev. B **35**, 120 (1987).
[36]V. I. Shnyrkov and S. I. Melnik, LTP **33**, 22 (2007) [Low. Temp. Phys. **33**, 15 (2007)].
[37]E. M. Lifshitz and L. D. Landau, *Statistical Physics: Course of Theoretical Physics*, 3rd ed. (Butterworth, London, 1984), Vol. 5, Chap. 12, p. 359.
[38]V. I. Shnyrkov, A. A. Soroka, A. M. Korolev, and O. G. Tutrutanov, LTP **38**, 382 (2012) [Low Temp. Phys. **38**, 301 (2012)].
[39]V. I. Shnyrkov, Th. Wagner, D. Born, S. N. Shevchenko, W. Krech, A. N. Omelyanchouk, E. Il'ichev, and H.-G. Meyer, Phys. Rev. B **73**, 024506 (2006).
[40]S. N. Shevchenko, Eur. Phys. J. B **61**, 187 (2008).
[41]V. I. Shnyrkov, A. M. Korolev, O. G. Turutanov, V. M. Shulga, V. Yu. Lyakhno, and V. V. Serebrovsky, LTP **41**, 1109 (2015) [Low Temp. Phys. **41**, 867 (2015)].
[42]A. M. Korolev, V. I. Shnyrkov, and V. M. Shulga, Rev. Sci. Instrum. **82**, 016101 (2011).
[43]E. Il'ichev and Ya. S. Greenberg, Europhys. Lett **77**, 58005 (2007).
[44]V. V. Danilov and K. K. Likharev, Tech. Phys. **45**, 1110 (1975).
[45]V. I. Shnyrkov and G. M. Tsoi, "Signal and noise, characteristics of RF SQUIDs," in *Principal and Applications of Superconducting Quantum Interference Devices*, edited by A. Barone (World Scientific, Singapore, 1992).
[46]A. M. Korolev, V. M. Shulga, I. A. Gritsenko, and G. A. Sheshin, Cryogenics **67**, 31 (2015).
[47]A. M. Korolev, V. M. Shulga, O. G. Turutanov, and V. I. Shnyrkov, Instrum. Exp. Tech. **4**, 37 (2015) [Instrum. Exp. Tech. **58**, 478 (2015)].

Translated by CWG